ABSTRACT

Title of Document:	AUTOMATION MODEL FOR pH AND CONDUCTIVITY ADJUSTMENT FOR A CATION EXCHANGE COLUMN ELUATE BUFFER
	Anupreet Parmar, Master of Science, 2010
Directed By:	Dr. William E. Bentley, Fischell department of Bio Engineering
	Dr. William A. Weigand, Chemical and Biomolecular Engineering

A comprehensive model for calculating pH and conductivity values for a buffer solution added to the eluate of a cation exchange column at Bayer Healthcare has been developed. Bayer Healthcare's Berkeley facility manufacturess Kogenate – a drug for Hemophilia. This project was carried out at one of the intermediate purification steps of Kogenate, where the pH and conductivity of a buffer solution added to a chromatographic column's eluate has to be critically adjusted. Currently this process is done manually and requires two operators. In order to reduce the manual labor as well as improve accuracy, an automation model was developed using feedback control and Bayer's pH and conductivity predicting empirical correlations.

AUTOMATION MODEL FOR pH AND CONDUCTIVITY ADJUSTMENT FOR A CATION EXCHANGE COLUMN ELUATE BUFFER

By

Anupreet Parmar

Thesis submitted to the Faculty of the Graduate School of the
University of Maryland, College Park, in partial fulfillment
of the requirements for the degree of
Master of Science
2010

Advisory Committee:
Dr. William Bentley
Dr. William Weigand
Dr. Ganesh Sriram

Table of Contents

List of Figures

Chapter 1: Automation Model at Bayer

Introduction

Bayer manufactures Kogenate, a drug used to treat hemophilia at the Berkeley, CA facility. Kogenate is recombinant factor VIII (rFVIII) used for treatment of Hemophilia A. rFVIII is produced by culture of mammalian cells derived from the BHK cell line (Baby Hamster Kidney, originating from the Syrian hamster) transfected with the human rFVIII gene. Kogenate is manufactured and purified at Bayer's Berkeley facility [2].

The experimental work for this project was carried between one of the intermediate purification steps where pH and conductivity of the product are required to be adjusted to a particular range. The details of the pH and conductivity adjustment process are given in the latter part of this chapter. The purification process of Kogenate is explained in the following paragraphs. Purification of Kogenate is divided into eight steps described as follows. Figure 1.1 shows a schematic of the entire process:

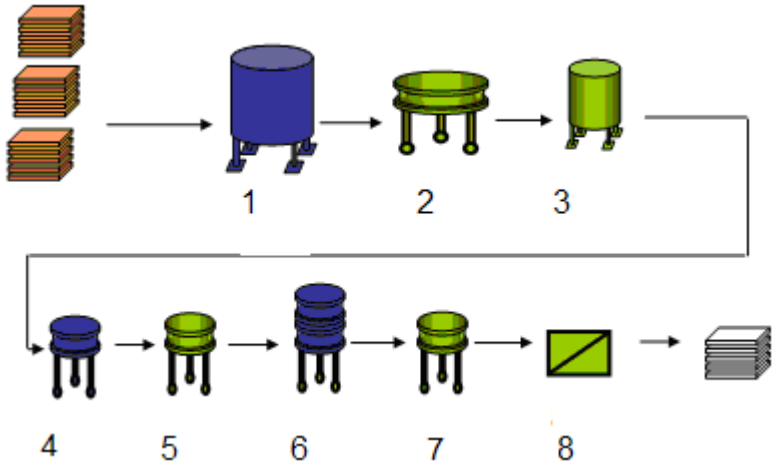

Figure 1.1: Schematic of purification process of Kogenate at Bayer Healthcare

Stage one is a thaw step. The tissue culture bags are left at the product processing temperature for thawing. After the product is thawed, it is filtered to remove any particulate matter. After that it is passed through an anion exchange column that is used to capture proteins including rFVIII. Impurities with a positive charge or a weak negative charge flow through the column and are collected as waste. Stage three is a viral inactivation step. A solvent detergent is used in this step to treat the solution which inactivates the viruses in it. The product is then passed through a series of four consecutive chromatographic columns to remove host cell impurities as well as any other contaminants. Stage seven is a filtration step that that basically reduces the volume of the product until now which is further diafiltered. [2]

Background

The eluate from stage six is called SP eluate which is mixed with an eluate buffer that is at a certain pH and conductivity. The pH and conductivity of the eluate buffer need to be readjusted before it is mixed with the stage 6 eluate. This adjustment is currently done manually with the help of operators. My project was to create a prototype for the automation of this adjustment step as described in the ensuing chapters.

The goal of the project was to come up with a prototype to automate the pH and conductivity of adjustment process for stage 6 eluate buffer before it is mixed with the eluate from column six and used in the next column. In this step, pH is adjusted from pH ~7.0 to pH 6.45-6.55 at 2-8° using 0.27M histidine and conductivity is adjusted from ~22 *mS/cm* to 17.15 *mS/cm* using water for injection (WFI).

Concept

Currently the pH is measured using Endress+Hauser Liquiline transmitter and Endress+Hauser Memosens probe [1]**.** In order to adjust the pH, initially 0.8 kgs of histidine is added to the eluate while the agitator is running. The solution is allowed to mix for about 3-20 minutes and the pH is measured again. The amount of histidine to be added again is calculated using equation (1.1):

$$Histidine\ to\ be\ added = \frac{pH_1 - 6.50}{0.318} \tag{1.1}$$

where pH_1 is the pH obtained after adding 0.8 kgs of histidine. Using this formula, batches of histidine are added until the pH falls with in the desired range. Its flow rate is adjusted manually based on real time pH measurements based on the operators'

experience. The entire process takes over an hour to complete and more importantly two operators are required simultaneously to operate the pump, do the pH calculations and monitor the pH. Figure 1.2 shows the flowchart of the current process.

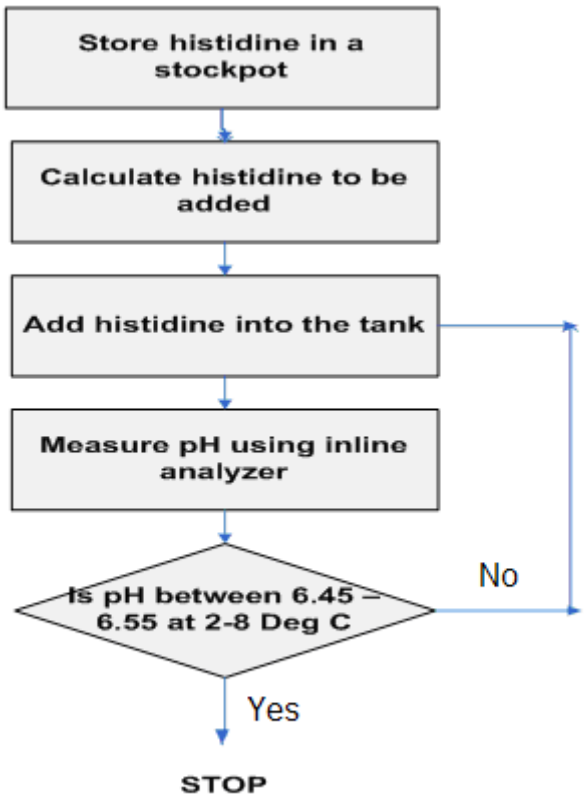

Figure 1.2: Current pH adjustment process overview

Since the goal of this project was to automate the addition of histidine to stage 6 eluate buffer in order to maintain the pH in the range of 6.45 – 6.55, a prototype for histidine addition to the buffer was developed using feedback control. In order to conduct the automation and for the DCS (Distributed Control System) to be able to control the equipment, the portable weighing scale used to measure histidine, pH transmitter and the pump used to pump histidine were connected to the DCS. Since

the DCS was in a different room from the experimental equipment, the wires had to be pulled through a conduit in the wall from purification suite to the trio block in a different room. Figure 1.3 shows the trio block that had 2 available input ports and 1 output port where the connections were made.

Figure 1.3: Trio block used make DCS connections to histidine weighing scale, pH transmitter and the pump

The pump, pH transmitter and the weighing scale accept 4 -20 mA signals. Through the trio block, the signals go to the LAN and finally to the DCS. A schematic of DCS connections is shown in figure 1.4. The DCS had two incoming signals and one outgoing signal shown as following:

- **Input Signals**
    - pH probe: The pH signal from the tank goes to the DCS and is used to calculate the amount of histidine to be added.
    - Weighing Scale: The weight signal from histidine scale goes to the DCS and is used to track the amount of histidine added.

- **Output Signal**
    - Pump: DCS sends a signal to the pump controlling the pump speed depending on the real time pH

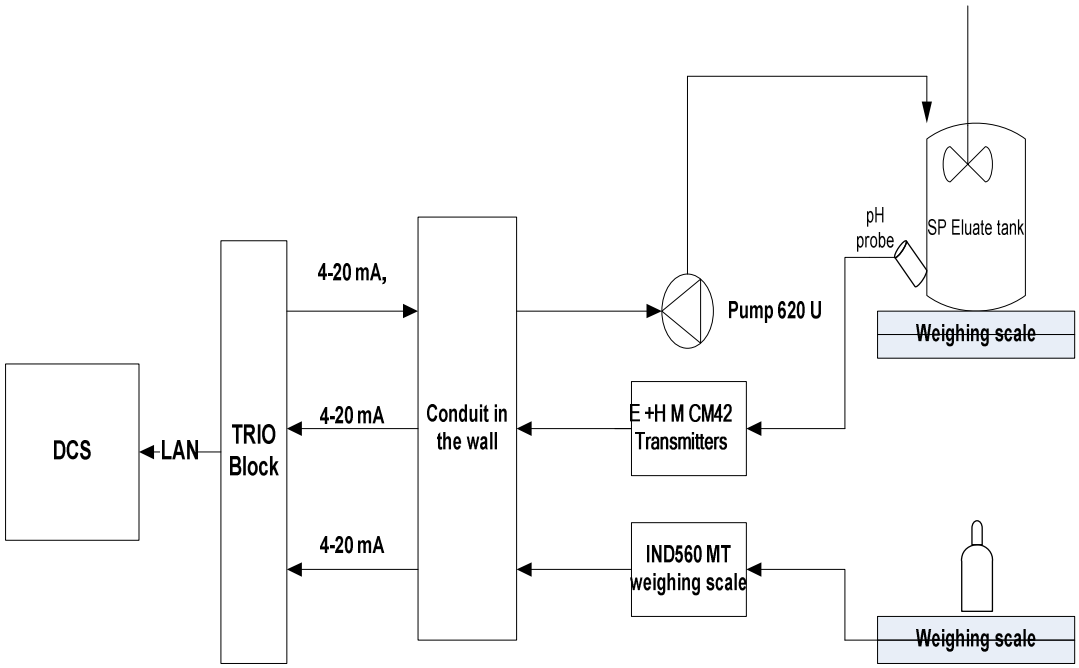

Figure 1.4: Figure showing the connections of pH probe, pump and weighing scale to the DCS

Process Requirements

Except for equipment, this section lists all the items required to perform stage 6 eluate adjustment operation

Stream	Stream Type
Stage 6 eluate	Core input
0.27 M Histidine	Subsidiary input

Table 1.1: Inputs and Outputs

Environmental Conditions

This operation was performed in a 2–8°C Cold room [2]. All solutions were 2–8°C. This is the industry standard for refrigeration temperature. The cool temperature is needed to keep the protein stable.

Equipment

Equipment
SP eluate tank
Floor Scale
Portable weighing scale
Carboy
pH meter
620 U Watson Marlow Pump

Table 1.2: Equipment list for pH adjustment automation experiment

Background Experiment

In order to make sure that the pH follows a smooth curve without any spikes around the target range, a pre-automation experiment was conducted to come up with a trend of change in the pH with manual addition of histidine. For this experiment, 65.2 kgs of eluate buffer was loaded into the stage 6 eluate tank and placed on the floor scale. The initial weight of the tank with the buffer was recorded and the scale was tared to 0. The initial temperature and pH of the solution were also recorded. The tubing connections were then made with end of the tube connected to the pump and the other

end connected to the histidine stockpot. The pump was then run at 20 revolutions per minute and the pH readings were recorded every 0.1 kg. However, this experiment was run until 2 kg of histidine was added to explore extreme additions to the solution. After the addition of 2 kg of histidine, the pump was stopped and the tubing was removed.

Figure 1.5 shows the plot of pH with histidine addition up to 2 kg. It turns out that pH follows a very linear curve in the range the experiement is conducted. Even though normally about 1.6-1.8 kg of histidine is required to bring the eluate back into the range, 2 kg of histidine was added to the eluate for this experiment to explore the case of overdilution. As seen in the curve, no sharp peak is seen as the histidine touches 2 kgs.

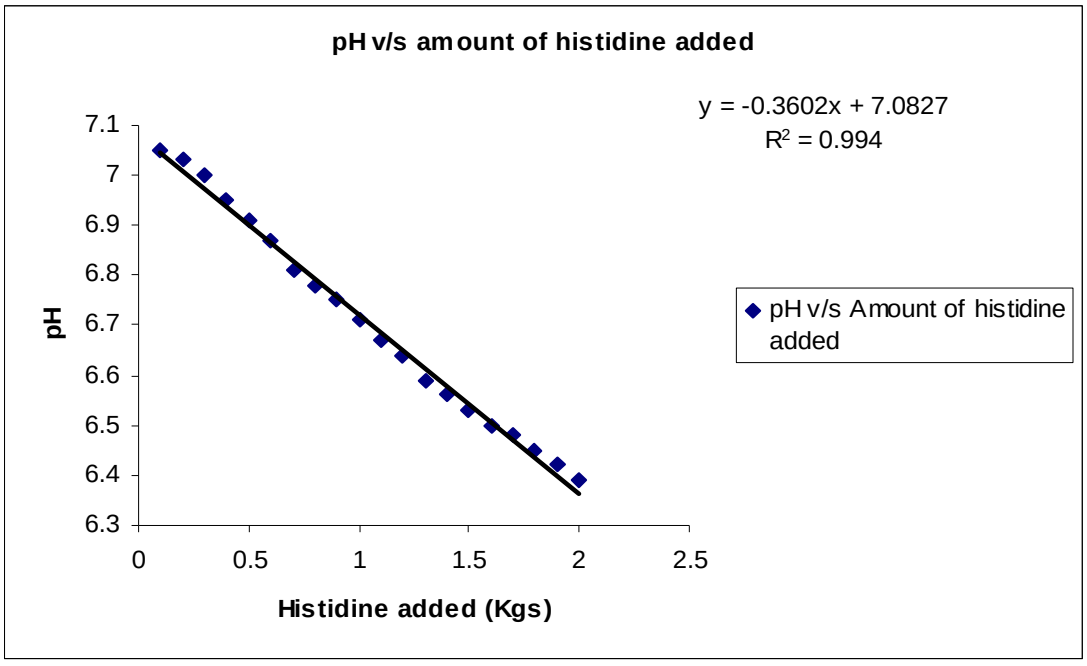

Figure 1.5: Plot of pH against the amount of histidine added

This plot was obtained for an initial buffer mass of 65.2 kg. The plot would be different for different initial buffer weights. Histidine was added manually and the

readings were taken after the values stabilized. Also, the above plots were taken at a starting buffer temperature of 4.6˚ C. After the stability of pH was confirmed in the operational range, the automation experiment was conducted.

Automation Algorithm

The stage 6 eluate buffer pH adjustment process was not designed to be fully automated. With the automation algorithm in place, it still required some manual intervention in order to keep a check on the pH. Since the pH range is narrow and the product at this stage is really expensive, any overdilution caused would cost a lot of money. Hence, it was made sure that the process was semi-automated so that the chances of missing the pH range are negligible. Figure 1.6 shows a flow chart of the automation algorithm.

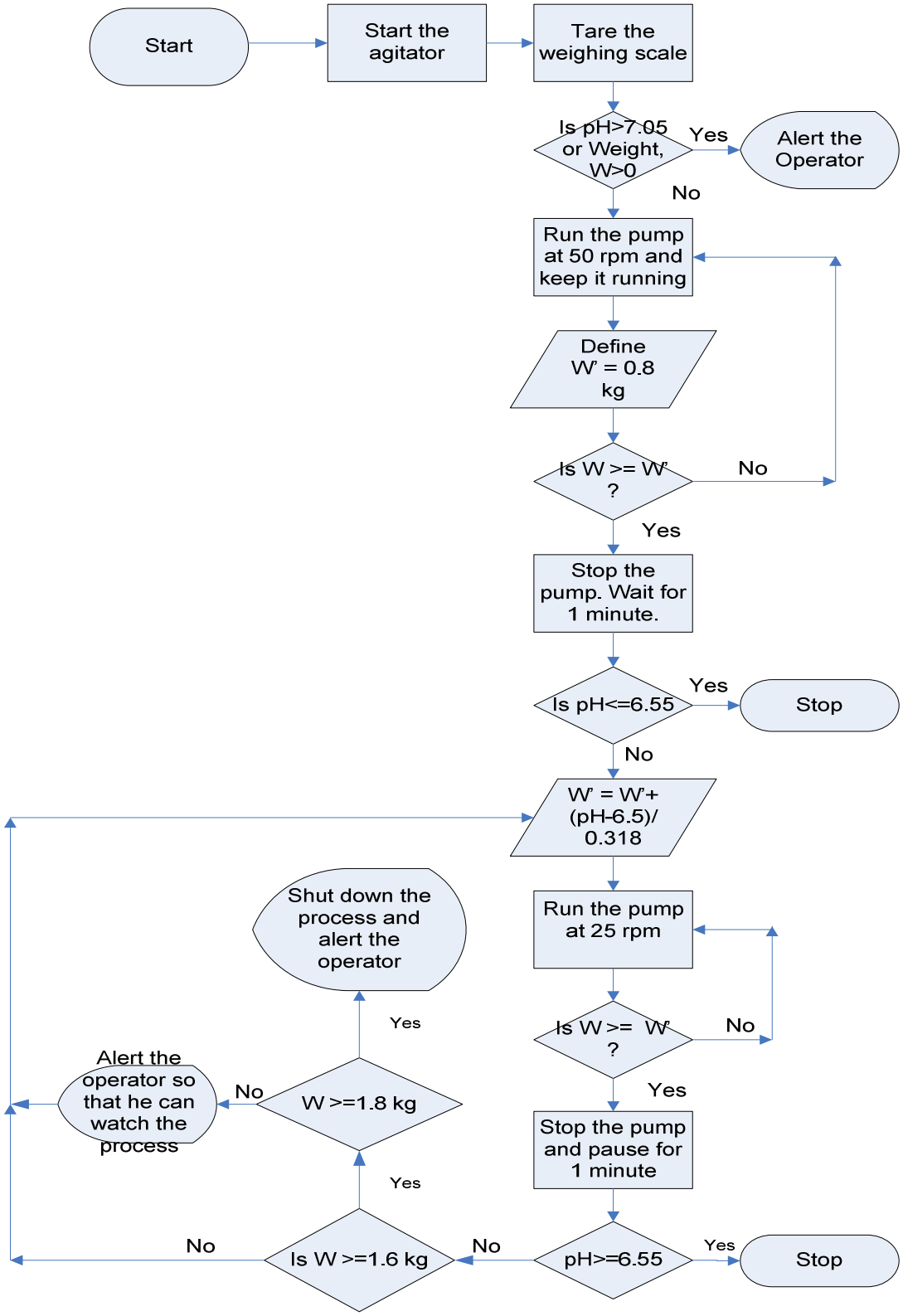

Figure 1.6: Flow chart of SP eluate automation

Procedure

For pH adjustment, the 0.27M histidine was placed on a portable calibrated scale in a plastic carboy. The tubing assembly was inserted into a peristaltic pump and the hose barb on the inlet side of the tubing was placed into the 0.27M histidine buffer. The tubing was purged of air using the histidine solution. The outlet-side of the tubing assembly was then connected to the tank inlet dipleg 3-way boss valve. The portable scale was tared to 0 and the tank inlet was opened. The peristaltic pump was started at 50 rpm until it had pumped 0.8 kg of histidine**.** Then the pump was stopped for 1 minute while the agitator continued to run at 26-28% agitator output. After a minute, the pump was started again at 25 rpm and the amount of histidine added was calculated using equation (1.1) as mentioned before

$$Histidine\ to\ be\ added = \frac{pH_1 - 6.50}{0.318} \tag{1.1}$$

where pH_1 is the pH obtained after adding 0.8 kg of histidine The same step was repeated and histidine was added until the pH fell in the desired range. When the total weight of histidine added was greater than 1.6 kg, the pump was stopped and the operator was alerted to confirm the proper working of the process. The operator checked the process for any discrepancies and removed the manual halt and continued the process. The algorithm was also designed to completely shut down the process in case the total weight of histidine added touched 1.8 kg, which did not happen in this experiment. The reason for this discrepancy has been discussed in the results section. By the end of the whole process, the pH was between 6.45-6.55 pH units.

Equipment Setup

Figure 1.7 shows the schematic of the stage 6 eluate buffer adjustment equipment setup. As seen in the diagram, the stage 6 eluate tank rests on the 0-1000 kg floor scale. The inline pH probe sends real time signal to the transmitter which in turn transmits the signal to the DCS. The DCS uses this signal to calculate the weight of histidine to be added to the eluate according to equation 1.1. Histidine rests on a portable ACME weighing scale which sends 4-20 mA weight signal to the DCS. This signal is used to track the amount of histidine left in the stockpot and the amount added to the eluate tank. The histidine is pumped into the tank using a 620U Watson Marlow pump[3]. The pump gets signal from the DCS according to which different speeds are set as mentioned in the procedure above. In general, the pump speed was kept very low so that the eluate buffer does not get overdiluted. There are both pros and cons of following such an approach. On one hand, the result is accurate and the solution never gets overdiluted, on the other hand it takes a lot of time if the pump speed is set really low. The agitator speed could be controlled by the DCS, but for this experiment, it was constant at 26-28% agitator output.

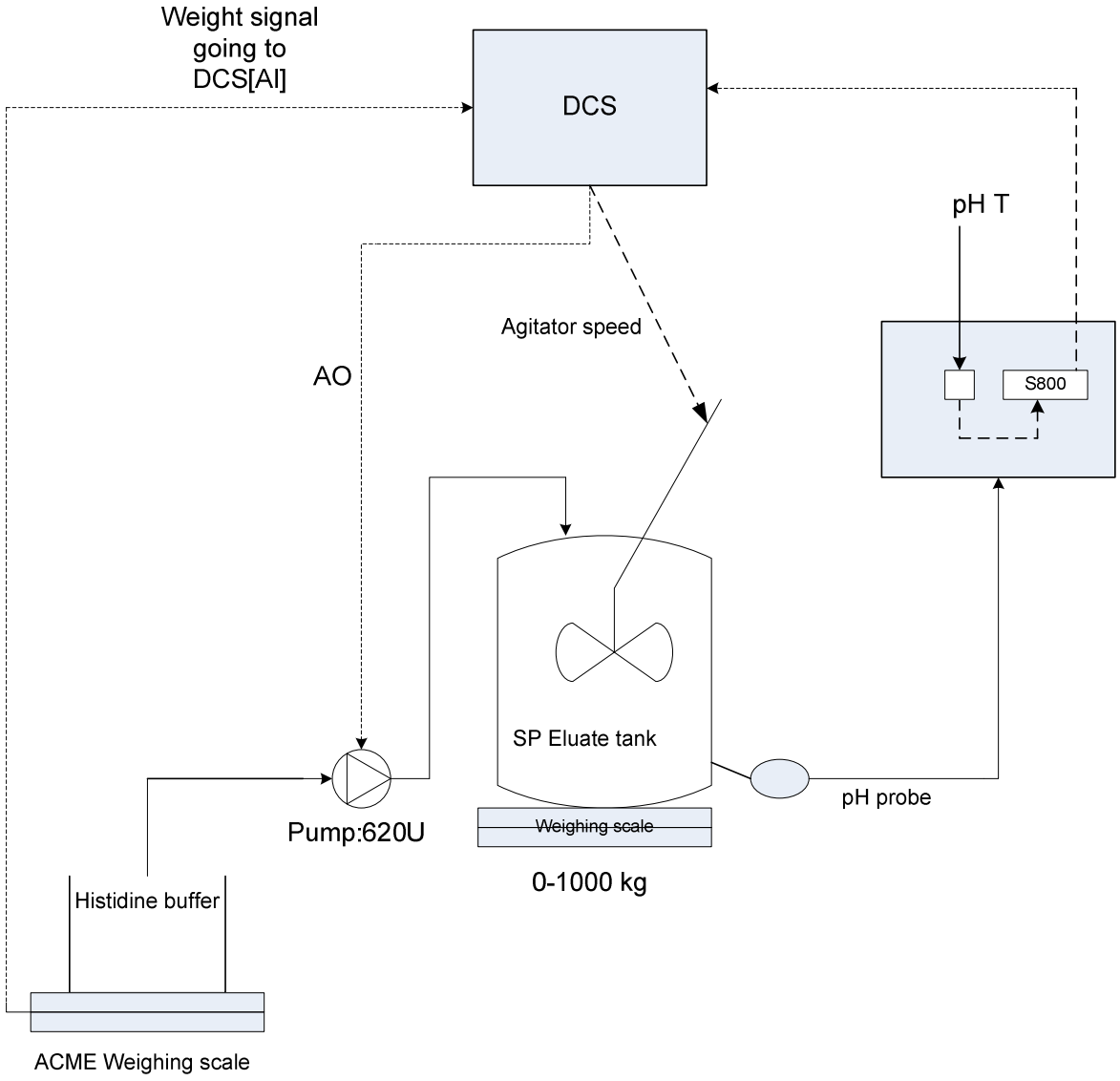

Figure 1.7 Equipment setup for SP eluate adjustment process

Results and Discussion

The proof of principle experiment for automation of the pH adjustment process was conducted successfully. The pH was adjusted between 6.45-6.55 in the three runs . Table 1.3 shows the amount of histidine added in the three runs for the final adjustment:

Run	Amount of histidine added (kg)
1	1.86
2	1.86
3	1.9

Table 1.3: **Amount of histidine added to for SP eluate pH adjustment**

Figure 1.8, 1.9 and 1.10 show the change in pH with the addition of histidine.

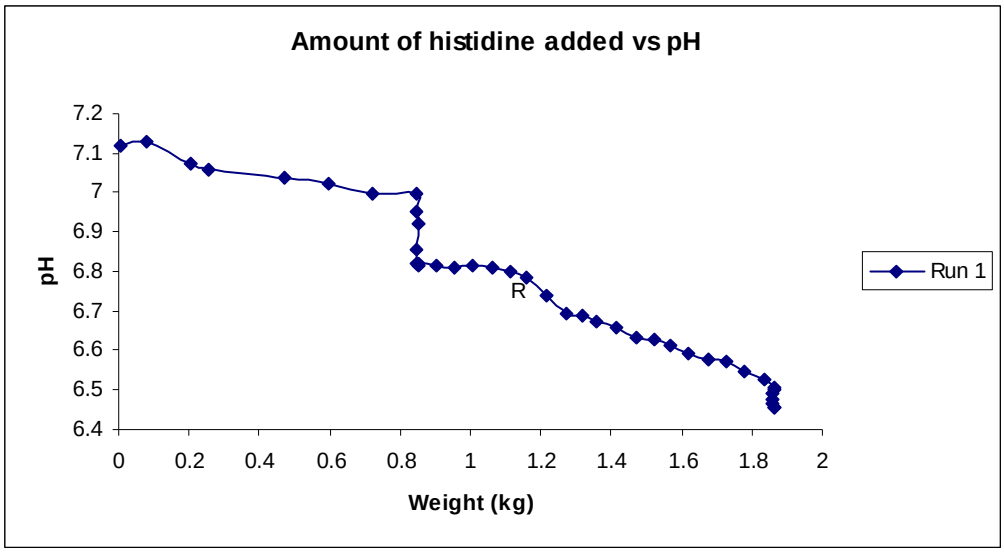

Figure 1.8: Plot showing the trend in pH with histidine addition for run1

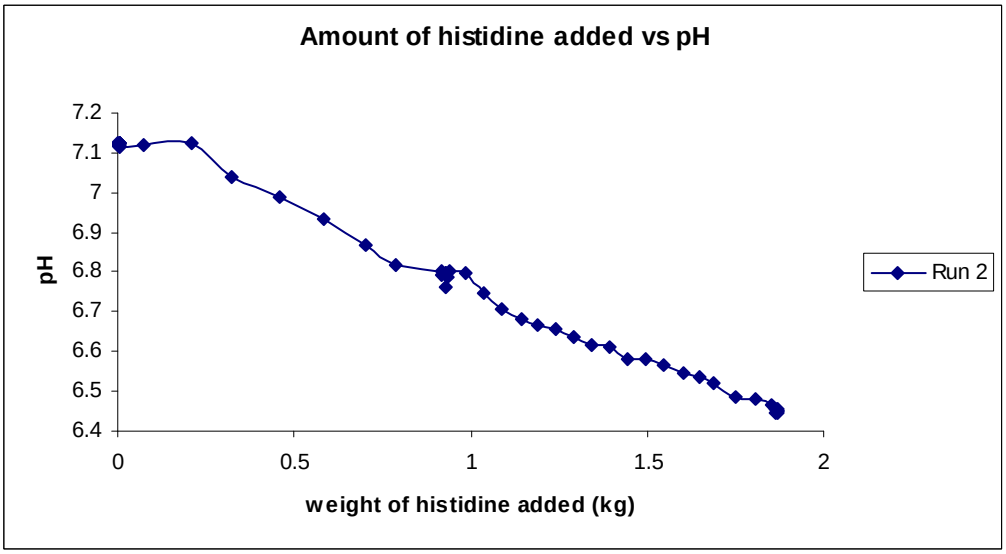

Figure 1.9: Plot showing the trend in pH with histidine addition for run 2

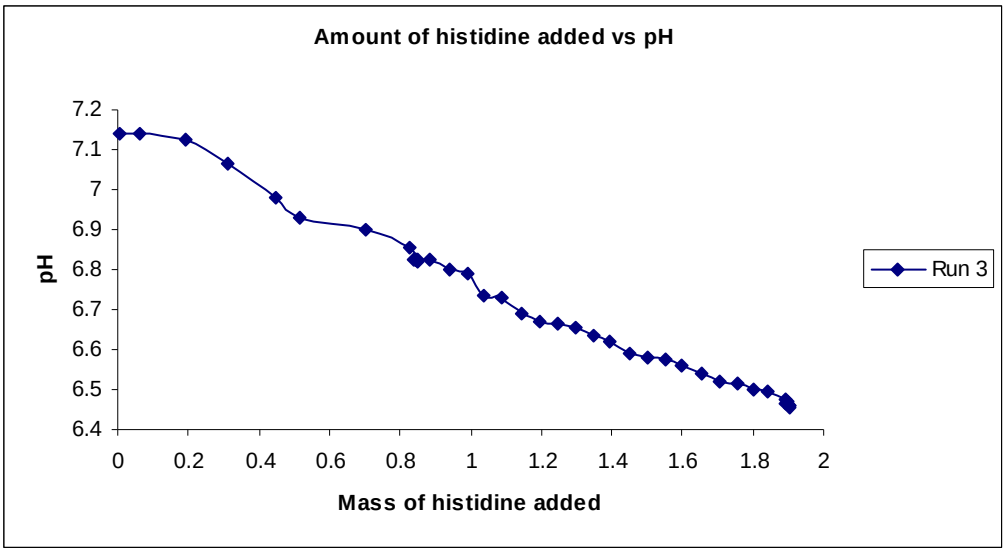

Figure 1.10: Plot showing the trend in pH with histidine addition for run 3

As seen in table 1.3, the weight of histidine added each time is greater than 1.8 kg. Historically, histidine amount used is equal or less than 1.7 kgs. However, for these runs, the starting pH was considerably high (>7.0), hence more histidine was used. Also, it is to be noticed that the algorithm states that if the histidine amount exceeds 1.8 kg the whole process should stop. However, in these tree runs, the pump adds ~1.9 kg histidine because after the second addition, the histidine amount is less than 1.8 kg. For the third addition, after the amount has been calculated, the pump gets the instruction from the DCS to pump the extra amount of histidine, which when added to the already added histidine exceeds 1.8 kg. Once the instruction has been given to the pump, it stops only after the full amount is added.

Conclusion

The proof of principle experiment for automation of stage 6 eluate adjustment process was successfully conducted. While the currently proposed model works well, there are improvements that can be made to improve the efficiency and accuracy of the process. This model used an empirical mass balance to calculate the amount of histidine to be added in each step. A more accurate theoretical model can be developed which will predict the pH with higher accuracy as well as precision. Stage 6 eluate contains imidazole which is basic. Histidine which is an acidic buffer is added to the eluate to bring down the pH. Ideally a pH model should be developed using the acid-base chemistry of these solutions to calculate the exact amount of histidine to be added to SP eluate in order to bring down the pH to desired range. Even the code used to run the experiment was very primitive. In order to get a better response, a finer process control model should be developed.

Also, this experiment was not fine tuned and did not have any graphics in the interest of time. For the actual automation, the DCS should have a separate module for SP eluate adjustment. Also, since the process is completely automated and no manual intervention occurs, the commands should be accompanied with alarms if something goes wrong. The drug at this stage is highly purified and is very valuable. Hence, losing even a small amount can cost a fortune.

The proof of principle experiment for the automation process was conducted successfully in the given time line. In order to implement this, a better and more accurate control model will be required to eliminate even the remotest possibility of overdilution.

Chapter 2: pH adjustment: A Theoretical approach

In the previous chapter , even though a successful working semi-automated pH adjustment process was developed, it lacked a supporting model that predicted the pH for varying amounts of histidine added. This chapter explores an empirical relationship developed between histidine mass and the pH of the stage 6 eluate solution.

Concept

Stage 6 eluate is made in a 150 L tank with the following composition:

Table 2.1: Component composition of stage 6 eluate[3]

Volume	**Component Concentration**	**Mass**
150 L	Imidazole = x 1.36 g/L	204 g
	NaCl = x17.53 g/L	2630 g
	$CaCl_2.2H_2O$ = X 6.36 g/L	954 g

An average batch of stage 6 eluate that undergoes pH adjustment is about 65 kg. The density of the solution is assumed to be 1 kg/L so a direct conversion of 65 kg to L is assumed hence forth in the model.

In order to bring down the pH, 0.27 M histidine is added to the eluate. Histidine is a triprotic acid[15]. Each batch of SP eluate on which the adjustment is done weighs about 65 L. So the number of grams of Imidazole in the batch are:

$$65\,L \times 1.36\frac{g}{L} = 88.4g \text{ of Imidazole} \qquad (2.1)$$

Molecular Mass of Imidazole[10] = 68.07 g/mol

Number of moles of Imidazole in the eluate buffer batch =

$$\frac{88.4\,g}{68.07\,\frac{g}{mol}} = 1.3 \text{ moles} \tag{2.2}$$

Let V be the volume of hisitidine added to completely react with 1.3 moles of imidazole. V can be calculated using the following equation for a triprotic acid:

$$1.3 \text{ moles} = 0.27\ \frac{moles}{L} \times 3 \times \text{V liters}$$

$$\text{V} = 1.6 \text{ L} \tag{2.3}$$

Assuming the density of the solution to be 1 g/cc, the weight of histidine to be added is 1.6 kg. Any histidine added beyond 1.6 kg would be treated as a buffer solution. Histidine is a triprotic acid [15][10]. Its dissociation can be shown from the following equations [6]:

$$H_3A + H_2O \rightarrow H_2A^- + H_3O^+ \qquad K_{a1} \tag{2.4}$$

$$H_2A^- + H_2O \rightarrow HA^{2-} + H_3O^+ \qquad K_{a2} \tag{2.5}$$

$$HA^{2-} + H_2O \rightarrow HA^{3-} + H_3O^+ \qquad K_{a3} \tag{2.6}$$

The above written equations can be manipulated to obtain the K_as of the following dissociation equations:

$$H_3A + H_2O \rightarrow H_2A^- + H_3O^+ \tag{2.7}$$

$$K_{a1} = \frac{[H_2A^-][H_3O^+]}{[H_3A]}$$

$$=> \ [H_2A^-] = \frac{K_{a1} \times [H_3A]}{[H_3O^+]} \tag{2.8}$$

$$H_3A \ + 2H_2O \rightarrow HA^{2-} \ + 2H_3O^+ \tag{2.9}$$

$$K_{12a} \ = \frac{[HA^{2-}][H_3O^+]^2}{H_3A}$$

$$=> \ [HA^{2-}] = \frac{K_{12a} \times [H_3A]}{[H_3O^+]^2} \tag{2.10}$$

$$H_3A + 3H_2O \ \rightarrow A^{3-} \ + 3H_3O^+ \tag{2.11}$$

$$K_{13a} \ = \frac{[A^{3-}][H_3O^+]^3}{[H_3A]}$$

$$[A^{3-}] = \frac{K_{13a} \times [H_3A]}{[H_3O^+]^3} \tag{2.12}$$

The total concentration of acid can be obtained from the following equation [9]

$$C_A = [H_3A] + [H_2A^-] + [HA^{2-}] + [A^{3-}] \tag{2.13}$$

Since all the imidazole has reacted initially with histidine (hence no leftover base), a charge balance on the species is shown in equation (2.14)

$$3[A^{3-}] + 2[HA^{2-}] + [H_2A^-] + [OH^-] = [H^+] \tag{2.14}$$

Also, the water ion product is written as follows

$$K_w = [H^+][OH \ ] \tag{2.15}$$

Hence, $[OH^-]$ in the equation (2.14) can be replaced by $\frac{K_w}{[H^+]}$

$$3[A^{3-}] + 2[HA^{2-}] + [H_2A^-] + \frac{K_w}{[H^+]} = [H^+] \tag{2.16}$$

where K_w is the water ionization constant . Equations (2.8), (2.10) and (2.12) can be used to replace the anions in equation (2.13).

$$C_A = [H_3A] + \frac{K_{a1} \times [H_3A]}{[H_3O^+]} + \frac{K_{12a} \times [H_3A]}{[H_3O^+]^2} + \frac{K_{13a} \times [H_3A]}{[H_3O^+]^3}$$

$$C_A = [H_3A] \times \frac{([H_3O]^3 + [H_3O]^2 \times K_{a1} + [H_3O] \times K_{12a} + K_{13a})}{[H_3O]^3}$$

$$\Rightarrow [H_3A] = \frac{C_A \times [H_3O^+]^3}{([H_3O]^3 + [H_3O]^2 \times K_{a1} + [H_3O] \times K_{12a} + K_{13a})}$$

(2.17)

Now equation (2.17) can be used to substitute for $[H_3A]$ in equations (2.8), (2.10) and (2.12) as shown in the following equations:

$$[H_2A^-] = K_{a1} \times \frac{C_A \times [H_3O^+]^2}{([H_3O]^3 + [H_3O]^2 \times K_{a1} + [H_3O] \times K_{12a} + K_{13a})}$$

(2.18)

$$[HA^{2-}] = K_{12a} \times \frac{C_A \times [H_3O^+]}{([H_3O]^3 + [H_3O]^2 \times K_{a1} + [H_3O] \times K_{12a} + K_{13a})}$$

(2.19)

$$[A^{3-}] = K_{13a} \times \frac{C_A}{([H_3O]^3 + [H_3O]^2 \times K_{a1} + [H_3O] \times K_{12a} + K_{13a})}$$

(2.20)

Plugging these equations back in (2.16), the following equation is obtained

$$\frac{3(K_{13a} \times C_A) + 2(K_{12a} \times C_A \times [H_3O^+]) + K_{a1} \times C_A \times [H_3O^+]^2}{[H_3O]^3 + [H_3O]^2 \times K_{a1} + [H_3O] \times K_{12a} + K_{13a}} + \frac{K_w}{[H_3O^+]} = [H_3O^+] \quad (2.21)$$

Here K_{a1} , K_{a2} , K_{a3} can be used from equations (2.1), (2.2) and (2.3) to obtain K_{12a} and K_{13a} as shown in the following equations:

$$K_{12a} = \quad K_{a1} \times K_{a2}$$

$$K_{13a} = \quad K_{a1} \times K_{a2} \times K_{a3}$$

Theoretically, equation (2.21) would be the ideal way to calculate the [H^+] ion concentration with the addition of histidine. However, the reaction does not take place at room temperature. The pH adjustment of the buffer is done at 4.6˚ C in the cold room. And since the K_a values of an acid depend on temperature [5], the dissociation constant at 4.6˚ C would be different from the ones readily available in literature. So the next best method was to empirically back calculate the K_a for the reaction.

In order to back calculate the empirical K_a for histidine, an experiment with manual histidine additions to the buffer was conducted. In this experiment, slow additions of histidine were made to the stage 6 eluate buffer solution and the respective pHs were recorded. This pH – histidine relationship was used to derive an effective K_a for the addition which is described in the latter part of this chapter. The procedure of the experiment is described as follows:

Procedure

1.1	Place the SP eluate tank on the weighing scale, record the initial weight and tare it to zero.
1.2	Record the temperature and initial pH of the solution
1.3	Start the agitator at 26-28% agitator output.
1.4	Connect one end of the pump tubing to the tank and the other end to the histidine stockpot.
1.5	Run the pump at 20 rpm.
1.6	Take pH readings every 0.1 kg up to 2 kgs.
1.7	Stop the pump.
1.7	Remove the pump tubing from histidine stockpot.

Results and Analysis

A plot of the amount of histidine added versus the pH is shown in figure 2.1

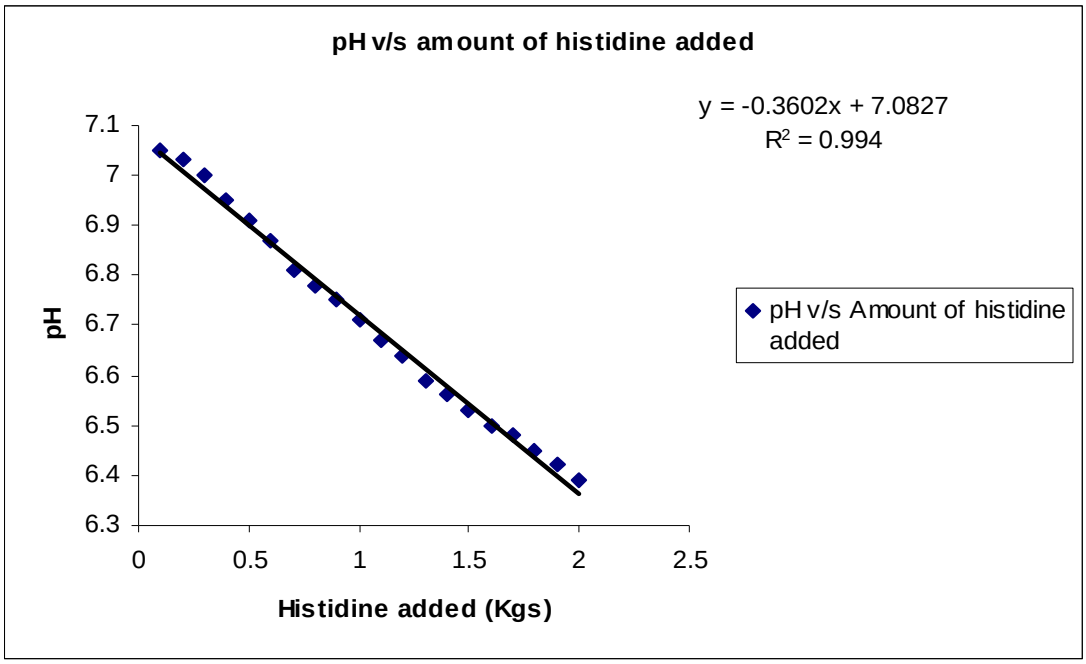

Figure 2.1: Plot of pH against the amount of histidine added

Mass of histidine to completely react with the imidazole present is calculated in equation (2.6). As mentioned above, it takes 1.6 kg of histidine to completely react with imidazole. Any extra addition of histidine would lead to a buffer solution formation governed by the following equation:

$$3\text{Imidazole} + 3H_3A \rightarrow A^{3-} + 3H_2O$$

From equation (2.2) above, total amount of imidazole available = 1.3 moles

Let the amount of histidine added (after 1.6 kg has been added already) = x kg

Total histidine added = 1.6 + x kg

Assume density of histidine = 1g/cc

Moles of excess histidine = (1.6+ x) L $\times$ 0.27 $\frac{moles}{L}$ = 0.27(x+1.6) moles

The above equation can be used to calculate

	3Imidazole	+	$3H_3A$	$\rightarrow$	A^{3-}	+	$3H_2O$
at time t	0 moles		$0.27(x+1.6) - \frac{1.3}{3}$ moles		$\frac{1.3}{3}$ moles		

At any time t (after imidazole has completely reacted), the concentration of the reactant and products can be calculated by using the following equation, where V = the volume of the solution already in the tank.

[Imidazole] = 0 M

$$[H_3A] = 0.27(x+1.6) - \frac{1.3}{3} \text{ moles} \times \frac{1}{V+(x+1.6)L} \quad (2.22)$$

$$[A^{3-}] = \frac{1.3}{3}\text{moles} \times \frac{1}{V+(x+1.6)L} \quad (2.23)$$

The left over histidine will make the solution act as a buffer. In order to simplify the buffer calculations, histidine is treated as a monoprotic acid and a 'net empirical overall Ka' is back calculated from the experimental data. The acid dissociation equation is shown in the following equation:

$$H_3A + H_2O \rightarrow H_2A^- + H_3O^+$$

$$K_a = \frac{[H_2A^-][H_3O^+]}{[H_3A]}$$

(2.24)

Here K_a is the first dissociation constant for histidine. Dissociation constant for water is further given by the following equation:

$$K_w = [H^+][OH^-]$$

Charge balance for the reaction can be written as follows:

$$[H_2A^-] + [OH^-] = [H^+] \qquad (2.25)$$

Also, $[H_3A] + H_2A^- = C_a$ (2.26)

At any time t, the total C_a can be calculated by evaluating equation (2.26) by using equations (2.22) and (2.23) as follows

$$C_a = (0.27(x+1.6) - \frac{1.3}{3} \text{ moles}) \times \frac{1}{V + (x+1.6)L} + \frac{1.3}{3} \text{moles} \times \frac{1}{V + (x+1.6)L}$$

$$= \frac{0.27 \times (x+1.6)}{V + (x+1.6)} \frac{moles}{L}$$, where x+1.6 is the total amount of histidine added.

$$= \frac{0.27 \times (Total\ Histidine\ added)}{V + (Total\ Histidine\ added)} \qquad (2.27)$$

Assuming dissociation of water to be negligible compared to the acid dissociation, equation (2.25) can be written as:

$$[H_2A^-] \approx [H^+] \tag{2.28}$$

Hence, equation (2.24) can be written as

$$Ka = \frac{[H_3O^+]^2}{[H_3A]} \tag{2.29}$$

Using equation (2.28), equation (2.26) can be rearranged to obtain the following equation:

$$[H_3A] = C_a - [H^+] \tag{2.30}$$

Inserting equation (2.30) in equation (2.29) we get

$$Ka = \frac{[H_3O^+]^2}{C_a - [H_3O]^+}$$

$$[H_3O^+]^2 + Ka[H_3O]^+ - Ka\,C_a = 0$$

$$[H_3O]^+ = \frac{-K_a + \sqrt{K_a{}^2 + 4K_aC_a}}{2}$$

(2.31)

Plugging in the values for C_a from equation (2.27) and fitting the $[H_3O]^+$ values from the experimental data into equation (2.31), an average Ka can be back calculated for the reaction.

$$K_a = 1.44 \times 10^{-11} \ \frac{mol}{L}$$

The calculated K_a was used to predict the pH values of the solution used for the automation experiment described in chapter 1 using equation (2.31).

Figure 2.2, 2.3 and 2.4 show the correlation between the predicted pH value and the actual value for the three runs.

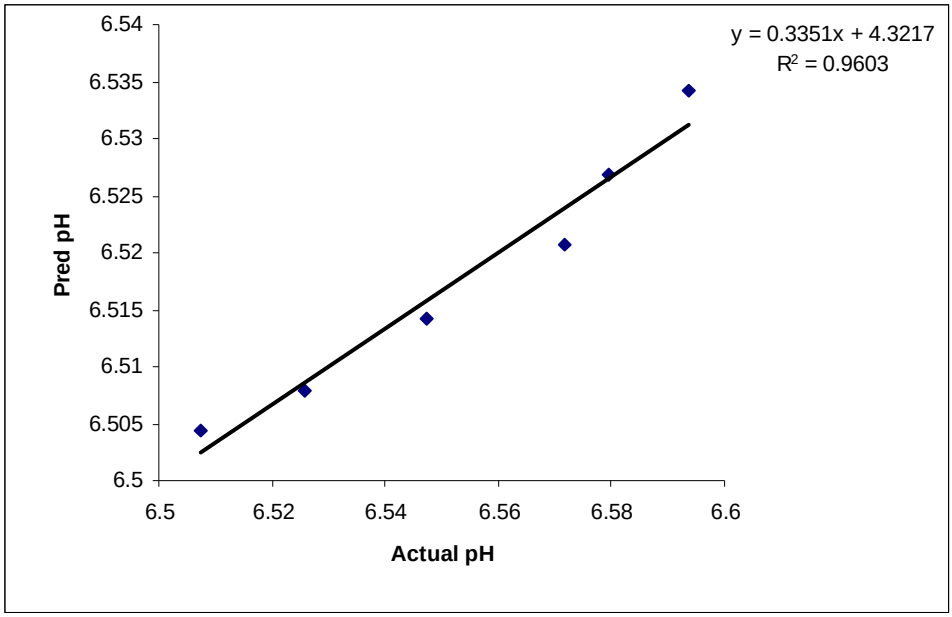

Figure 2.2: Plot of the predicted pH values using the theoretical K_a versus the actual pH values for run 1 of the automation run

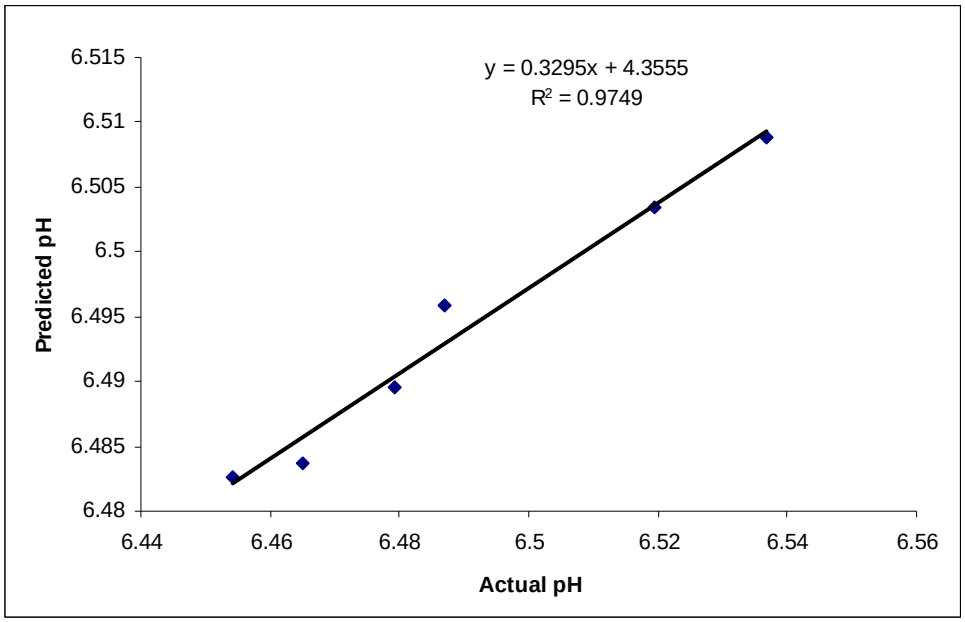

Figure 2.3: Plot of the predicted pH values using the theoretical K_a versus the actual pH values for run 2 of the automation run

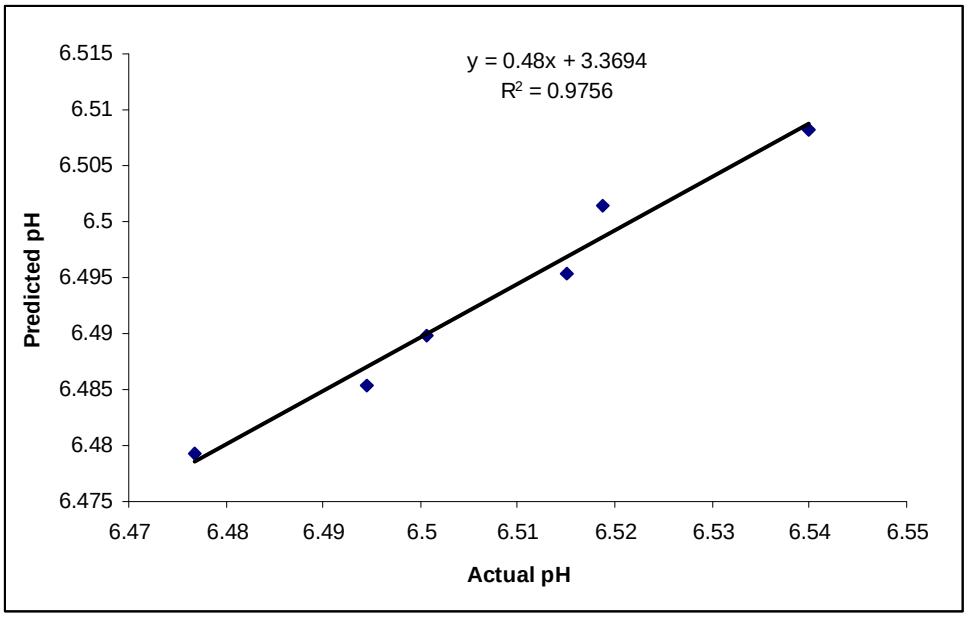

Figure 2.4: Plot of the predicted pH values using the theoretical Ka versus the actual pH values for run 3 of the automation run

Conclusion

As seen in the above plots, the empirically derived K_a predicts the pH values fairly well. However, this model was not used for the automation process developed in chapter 1 because the product at the sixth stage is really expensive and there is no tolerance for over or under-dilution of the buffer solution. So in order to prevent over-dilution, the empirical pH predicting model developed by Bayer was used for the automation since that model always undercalculates the amount of histidine to be added. However, Chapter 4 of this report does discus the future work that can be done using the pH model developed in this chapter.

Chapter 3: Conductivity Adjustment: A Theoretical Approach

Conductivity is the ability of a solution to transfer electric current. At Bayer it is an indirect way of measuring the concentration of dissolved solids. After the pH is adjusted using histidine, the next step is conductivity adjustment. Bayer uses Cold Water for Injection (CWFI) to bring down the conductivity of the incoming eluate buffer to the desired range.

WFI is an ultra purified form of water that is produced by distillation or reverse osmosis[16]. The conductivity of WFI used at Bayer lies in the range of 0.3 $\mu S / cm$ to 0.8 $\mu S / cm$ [3]. A Mettler-Toledo M700 Transmitter & 7108 Probe are used to measure the conductivity inline in the stage 6 eluate buffer tank and obtain real time measurements. The adjustment is conducted at about 5 degrees C in the cold room. In order to account for any subtle change in temperature the conductivity meter uses temperature compensation.

The incoming eluate after pH adjustment has a conductivity of the range 22 mS/cm [3]. The accepted range for SP eluate conductivity before it goes to the next chromatographic column is 17.0 – 17.30 mS/cm. Conductivity of the eluate is currently adjusted manually using the following equation[3]:

$$W_0 \times C_0 = W_1 \times C_1 \tag{3.1}$$

where W_0 is the incoming eluate buffer weight, C_0 is the conductivity of the incoming pH adjusted solution, W_1 is the total weight of the eluate after CWFI is

added and C_1 is the conductivity of the solution after CWFI is added. The conductivity of the solution is always undercalculated using the above equation. So procedure is repeated until the conductivity falls in the desired range. Figure 3.1 shows the flowchart of the adjustment process:

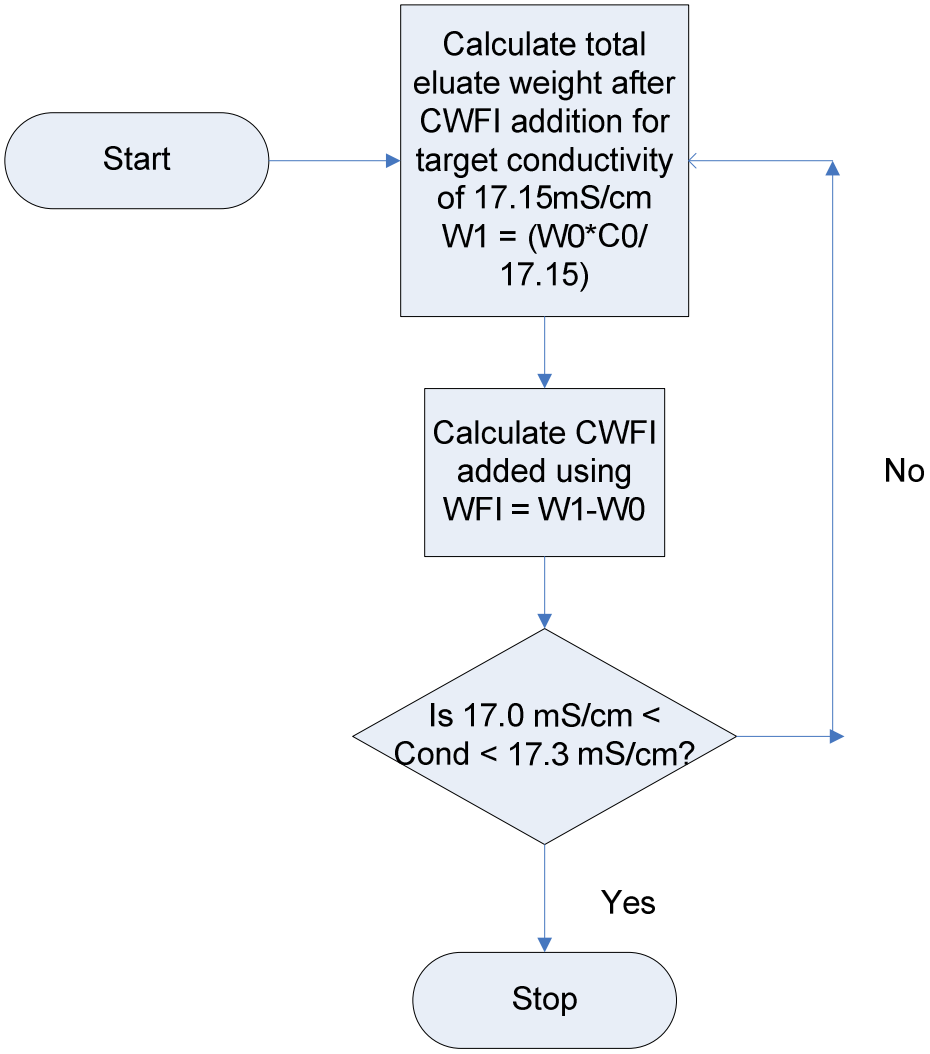

Figure 3.1: Flow chart of the current conductivity adjustment step

An inline conductivity meter is used to measure the conductivity of the eluate. Currently, the addition is done using multiple discrete additions which requires operator experience and excellence. Operators calculate the amount of WFI to be

added using equation (3.1) and the conductivity meter is checked for real time values. If the conductivity falls with in the acceptable range, the process is stopped or else the calculation is done again and the process is repeated until the desired conductivity is achieved.

Area for improvement

The current method of adjustment follows a trial and error technique to reach the target conductivity. Equation (3.1) basically extrapolates the conductivity of the solution assuming a linear model based on the mass of the solution. While equation (3.1) gives a ballpark figure of the amount of WFI to be added, it does not exactly calculate the total amount. This chapter explores a model that uses Kohlrausch's law to predict the solution conductivity correlating it to the mass of CWFI added. Kohlrausch's law basically relates the concentration of a solution to its conductivity. In the following paragraphs, Kohlrausch's law has been explored to obtain a process model for estimating the stage 6 eluate buffer conductivity.

Theory

Kohlrausch's Law of independent migration of ions states that the conductivity of a solution is composed of separate contributions from each of its constituent ions [8]. Consider an electrolyte $A_{\nu+}B_{\nu-}$ that dissociates into its respective ions as shown in equation (3.2)

$$A_aB_b \rightarrow aA^{b+} + bB^{a-} \qquad (3.2)$$

Molar conductivity for the A_aB_b would be given by equation (3.3)

$$\lambda = a\lambda_A + b\lambda_B \tag{3.3}$$

Equation (3.3) is useful when exact conductivity of a given solution has to be calculated. In this case, the incoming conductivity of the solution is known. WFI with conductivity $0.5\,\mu S/cm$ to $0.8\ \mu S/cm$ is added to the buffer to bring down the conductivity. Since the amount of solute in the solution is constant, a second form of Kohlrausch's law can be used to predict the conductivity after the WFI is added.

In this form, molar conductivity λ of an electrolyte at sufficient dilution is a linear function of the root of its concentration c [4]. Equation (3.4) shows the equation governing Kohlrausch's law

$$\lambda_c = \lambda_\infty - K\sqrt{c} \tag{3.4}$$

where λ_c is the conductivity at concentration c, λ_∞ is the conductivity of the solution at infinite dilution and c is the electrolyte concentration.

In this case, the solution is diluted by adding WFI to it. Conductivity before and after dilution can be calculated using the following equations:

$$\lambda_1 = \lambda_\infty - K\sqrt{c_1} \tag{3.5}$$

$$\lambda_2 = \lambda_\infty - K\sqrt{c}_2 \tag{3.6}$$

Where

λ_1	Molar conductivity before dilution
λ_2	Molar conductivity after dilution

c_1	Concentration before dilution
c_2	Concentration after dilution
K	Kohlrausch's constant

Equation (3.6) can be subtracted from equation (3.5) to obtain equation (3.7) as follows:

$$\lambda_2 - \lambda_1 = K(\sqrt{c_1} - \sqrt{c_2}) \tag{3.7}$$

Now λ_2 can be calculated from this equation

$$\lambda_2 = \lambda_1 + K(\sqrt{c_1} - \sqrt{c_2}) \tag{3.8}$$

However, $c = \frac{n}{V}$, where n is the number of moles of the electrolyte and V is the total volume of the solution. Evaluating c in equation (3.8), the following equation is obtained:

$$\lambda_2 = \lambda_1 + K(\sqrt{\frac{n_1}{V_1}} - \sqrt{\frac{n_2}{V_2}}) \tag{3.9}$$

But $n_1 = n_2 = n$, since the amount of electrolyte in the solution is constant and only water is being added to dilute it. Hence, equation (3.9) be written as

$$\lambda_2 = \lambda_1 + K \times n\,(\sqrt{\frac{1}{V_1}} - \sqrt{\frac{1}{V_2}}) \tag{3.10}$$

$$\lambda_2 = \lambda_1 + k\,(\sqrt{\frac{1}{V_1}} - \sqrt{\frac{1}{V_2}}) \tag{3.11}$$

where k is the modified Kohlrausch's constant.

Assuming the density of the solution to be 1g/cc, volume in equation (3.11) can be replaced by the mass of the solution.

$$\lambda_2 = \lambda_1 + k\left(\sqrt{\frac{1}{m_1}} - \sqrt{\frac{1}{m_2}}\right) \tag{3.12}$$

Equation (12) can be rearranged to give equation (13)

$$\sqrt{\frac{1}{m_2}} = \sqrt{\frac{1}{m_1}} - \frac{(\lambda_2 - \lambda_1)}{\mathrm{k}}$$

$$m_2 = \frac{m_1 k^2}{(k - \sqrt{m_1}\lambda_2 + \sqrt{m_1}\lambda_1)^2} \tag{3.13}$$

With the target conductivity λ_2 known, the amount of WFI can be calculated, where the amount of WFI to be added: $m_2 - m_1$

Implementation and Results

The result in equation (3.13) can be used to calculate the amount of WFI to be added to achieve the target conductivity. However, in order to implement equation (3.13), the modified kohlrausch constant should be calculated for this solution.

WFI addition data for the year 2008 is available. Table 3.1 shows the WFI addition data for January and February of 2008.

Lot	Cond 1 (mS/cm)	M1 (kg)	WFI added	Cond 2 (mS/cm)	M2 (kg)
1	22.2	64.3	21.3	17.2	85.6
2	21.6	64.2	18.5	17.1	82.7
3	21.9	64.5	19.7	17.2	84.2
4	22	65.3	20.3	17.2	85.6
5	21.9	65.2	19.9	17.2	85.1
6	22	65.4	20.3	17.1	85.7
7	21.4	65.3	17.5	17.2	82.8
8	21.8	65.2	20	17.1	85.2
9	22.8	67.4	22.7	17.2	90.1
10	21.3	67	18.4	17.1	85.4

11	20.6	67.2	15.6	17.2	82.8
12	21.8	65.3	20	17.2	85.3
13	21.6	65.9	20.4	17.2	86.3
14	21.8	65.4	20.1	17.1	85.5

Table 3.1: Data showing the WFI addition and the respective final conductivities for the month of February and January

Data until June end was used to derive a correlation between equation (3.13) and the data and the modified kohlrausch's constant, *k* was obtained. The following *k* was obtained from the above calculations:

$$k = -306.66 \frac{mS}{cm}\sqrt{kg} \qquad (3.14)$$

This *k* was used to predict the mass of WFI to be added. The results are shown in figure 3.2 and 3.3.

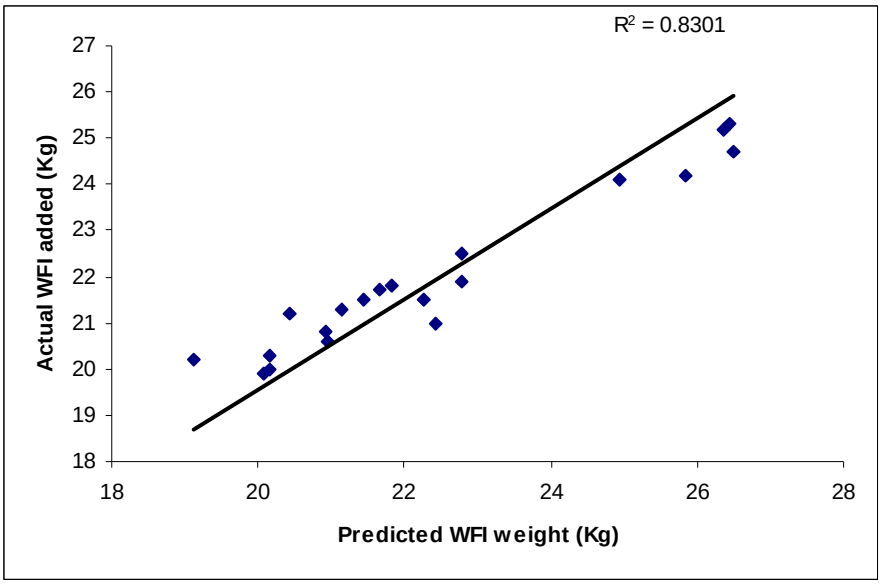

Figure 3.2: A plot of actual WFI added v/s predicted WFI to be added to achieve the target conductivity

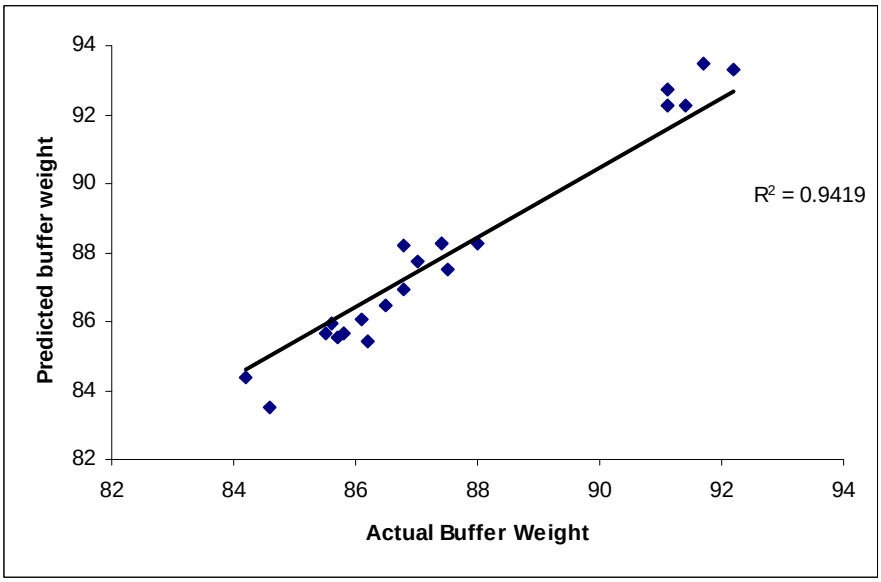

Figure 3.3: Plot of the predicted buffer weight (buffer + added WFI) vs the actual buffer weight

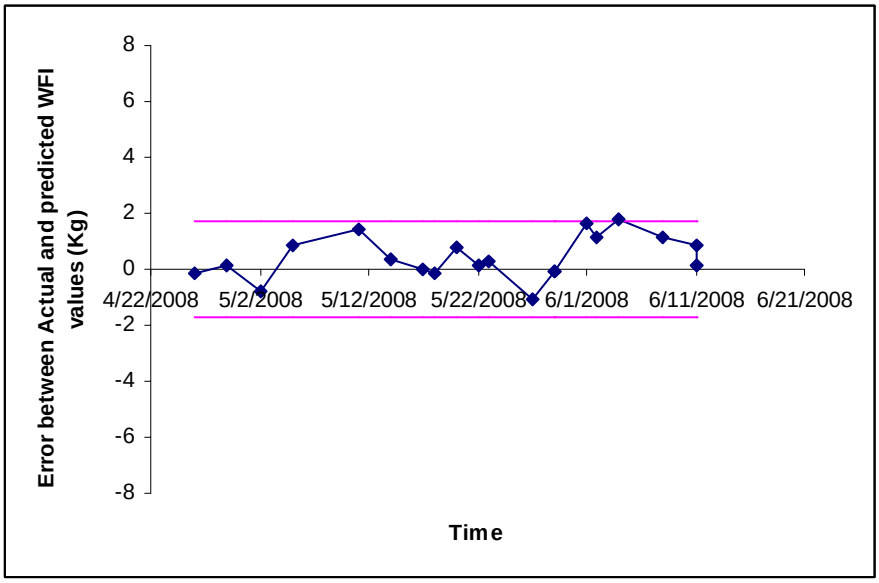

Figure 3.4: A plot of the difference between the predicted and actual WFI to be added to the buffer to achieve the target conductivity

As seen in figure 4, the mean of the difference in the predicted mass of WFI and the actual WFI added to achieve the target conductivity is 0.65 kg with a minimum error seen in this data is 0.029 kg and the maximum error is 1.79 kg. The average WFI added during the span of the data is 21.99 kg. So the percentage range of the error can be calculated as follows:

$$\frac{0.029}{21.99}\times 100\% \le error \le \frac{1.79}{21.99}\times 100\%$$

$$\Rightarrow 1.3\% \le \text{Error} \le 8.41\%$$

The error calculated is not that huge but considering Bayer's requirement of zero tolerance for error, the model could be further worked upon in the future and improved.

Conclusion

Kohlrausch's law can be used to calculate the amount of WFI to be added if the target conductivity is known with the maximum variation of about 8.41 %. One of the sources of errors in this conductivity calculation is the dependence of the conductivity on temperature[1]. The cold room's temperature fluctuates from anywhere between 2-8˚ C. Reproducing the same WFI mass at different temperature definitely would not be possible.

Even though a completely automated model would be wonderful for Bayer's use, there is zero tolerance for over or underdilution of the stage 6 buffer solution. Hence, in the following sections of this chapter, a conductivity automation model is developed that is based on their current conductivity predicting model.

Process Control Implementation

The automation of pH adjustment process was carried out successfully at Bayer Healthcare using feedback control. A similar automation model can be developed for conductivity using Bayer's existing conductivity predicting equation. A feedback control process on similar lines of the pH adjustment process can be developed since the former model proved to work successfully.

However, this chapter discusses three other types of feedback control models - proportional control, proportional integral control and proportional integral derivative control. Since the final conductivity needs to be in *17.0 – 17.3 mS/cm* range so the set point is defined to be an average of these two numbers - *17.15 mS/cm* .

As described in the equations (3.1) conductivity can be calculated using equation (3.15)

$$\lambda = \frac{\lambda_0 \times m_0}{m} \tag{3.15}$$

Here λ_0 is the former conductivity of the solution, m_0 is the former mass of the solution, m is the instantaneous (new) mass of the solution after the addition of WFI.

This mass can be obtained by doing a mass balance on the SP eluate tank as follows:

Accumulation = Input – Output + Generation – Consumption

$$\frac{dm}{dt} = F_{in} - 0 + 0 - 0 \tag{3.16}$$

Equation (3.16) can be rearranged to evaluate m as shown in the following equation

$$m = \int F_{in}\, dt \tag{3.17}$$

Equation (3.15) and (3.16) can be used to obtain the conductivity based on the flow rate of WFI. Now the control model to calculate the flow rate based on the feedback of the error in conductivity will be developed in the following sections. The following part of the chapter discusses three control approaches – Proportional control, Proportional Integral Control and Proportional Integral Derivative control.

Proportional Control

Proportional control is the simplest type of controller discussed in this report. For proportional control, the control effort is always proportional to the error in the system. The governing equation for proportional control can be obtained as follows[13]:

Control Effort =Proportional Gain $\times$ *Error*

$$P_{out} = K_p \times \xi(t) \tag{3.18}$$

where P_{out} is the output of the proportional controller, K_p is the proportional gain, and $\xi(t)$ is the instantaneous error.

In the case of conductivity adjustment, P_{out} is the controlled variable which is the instantaneous flow rate of WFI, *F(t),* and $\xi(t)$ is the difference (error) between the instantaneous conductivity and the set point. Since the target conductivity range to be reached is *17.0 – 17.3 mS/cm* , the setpoint λ_{SP} is set to the average of the two numbers – *17.15 mS/cm.* In this case, equation (3.18) can be written as

$$F(t) = K_p \times (\lambda(t) - \lambda_{sp}) \tag{3.19}$$

Equations (3.15), (3.17) and (3.19) can be solved numerically and $\lambda(t)$ can be obtained over time and plotted in figure 3.5 and 3.6:

Figure 3.5 shows the decrease in the instantaneous error - $\xi(t)$ with time using proportional control.

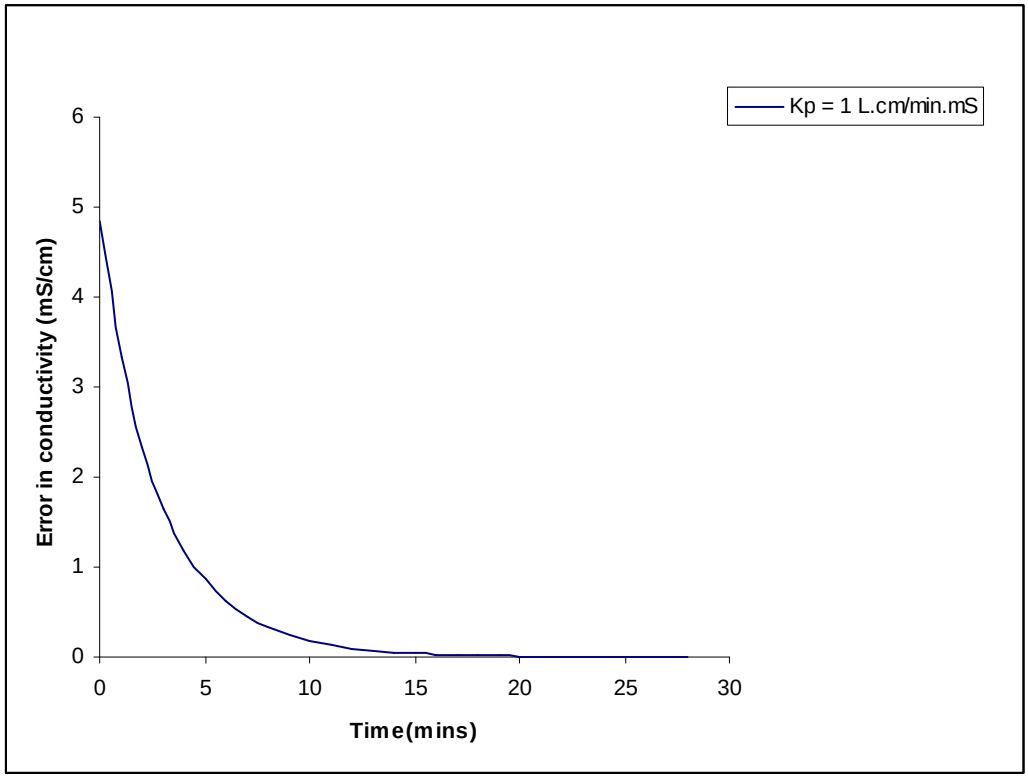

Figure 3.5: A plot showing the change in instantaneous error $\xi(t)$ over time

Using the instantaneous error $\xi(t)$, the instantaneous conductivity $\lambda(t)$ can be calculated. Figure 3.6 shows the plot of $\lambda(t)$ with time.

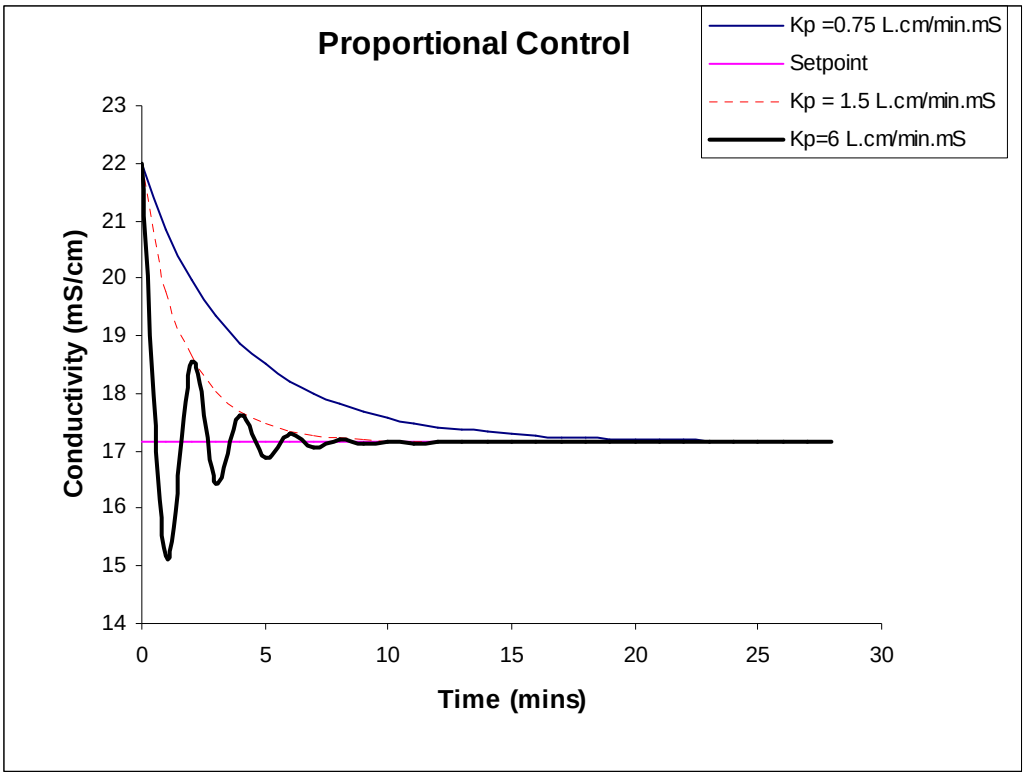

Figure 3.6: Plot of conductivity of stage 6 eluate buffer solution with time

For proportional control, as K_p increases, the setpoint is reached quicker[11]. Figure 3.6 clearly illustrates that point - as the K_p increases, the conductivity approaches its target value much quickly. The higher the K_p value, the faster the $\lambda(t)$ value approaches the set point value. However, the value of K_p can not be increased infinitely as the system becomes oscillatory which is a sign of an unstable system[14]. This concept can again be illustrated in figure 3.6. When K_p is 0.75 and 1.5 $\frac{L.cm}{\min.mS}$ the conductivity approaches the set point in a smooth fashion. However, when the K_p is increased to 6 $\frac{L.cm}{\min.mS}$, the oscillatory behavior starts to kick in. So

the right parameters have to be tuned experimentally and an optimum upper limit has to be established at Bayer, which could be part of the future work there.

Proportional Integral Control

As seen in the above plots, the set point is approached asymptotically using proportional control. While proportional control only uses the instantaneous error for the calculation of the output variable, integral control uses the history of error over time[14]. In integral control, the control signal depends on the sum of errors over a particular interval of time. Normally, the proportional and integral control are used in parallel known as PI control. The representative equation for PI control is given as follows:

$$P_{out} = K_p \times \xi(t) + K_I \int_0^t \xi(t)dt \tag{3.20}$$

In this case, the output variable – flow rate can be written in terms of equation (3.20) as follows:

$$F(t) = K_p \times (\lambda(t) - \lambda_{sp}) + K_I \int_0^t (\lambda(t) - \lambda_{sp})$$

The above written equation can be rewritten in its discrete form for the ease of numerical calculations[12]:

$$F_k = K_p \times (\lambda_k - \lambda_{sp}) + K_I \Delta t \sum_{i=1}^{k} (\lambda_k - \lambda_{sp}) \tag{3.21}$$

Solving equation (3.21) along with equations (3.15) and (3.17) numerically, the trend of conductivity over time can be plotted using PI control. In this plot, K_p is left constant at 1 $\frac{L.cm}{\min .mS}$ and K_I is varied as shown in figure 3.7:

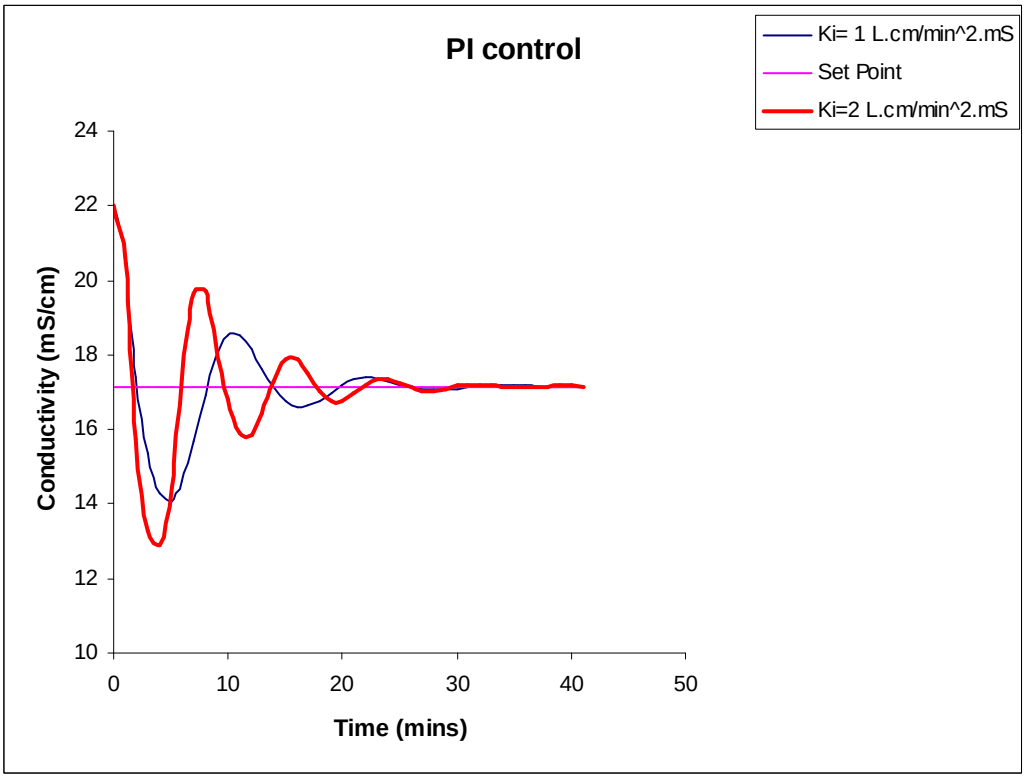

Figure 3.7: Plot of conductivity of stage 6 eluate buffer over time using PI control for different K_I s

Figure 3.7 illustrates this concept well because as seen, the conductivity oscillates for a while before it actually reaches the set point. The next section illustrates PID control for the same adjustment step.

Proportional Integral Derivative Control

PID control has the advantages of proportional and integral control clubbed with the derivative control. The derivative action is calculated based on the feedback measure

of the rate of change of the error signal. If the error is increasing at a higher rate, it will send a greater feedback signal in order to do the corrective action and bring back the value to the set point. Overall it stabilizes the process by providing an anticipatory control action.

Derivative control is mostly used along with PI control in the form of PID control. Thus for PID action, the representative equation can be written as follows:

$$P_{out} = K_p \times \xi(t) + K_I \int_0^t \xi(t)dt + K_d \frac{d\xi(t)}{dt} \quad (3.22)$$

In this case the controller output is the flow rate which is given by the following equation:

$$F(t) = K_p \times (\lambda(t) - \lambda_{sp}) + K_I \int_0^t \lambda(t) - \lambda_{sp}) \quad + K_d \frac{d(\lambda(t) - \lambda_{sp})}{dt}$$

(3.23)

Solving equation (3.15), (3.17) and (3.23) simultaneously, λ can be obtained as a function of time. Figure 3.8 shows the graph of λ over time t:

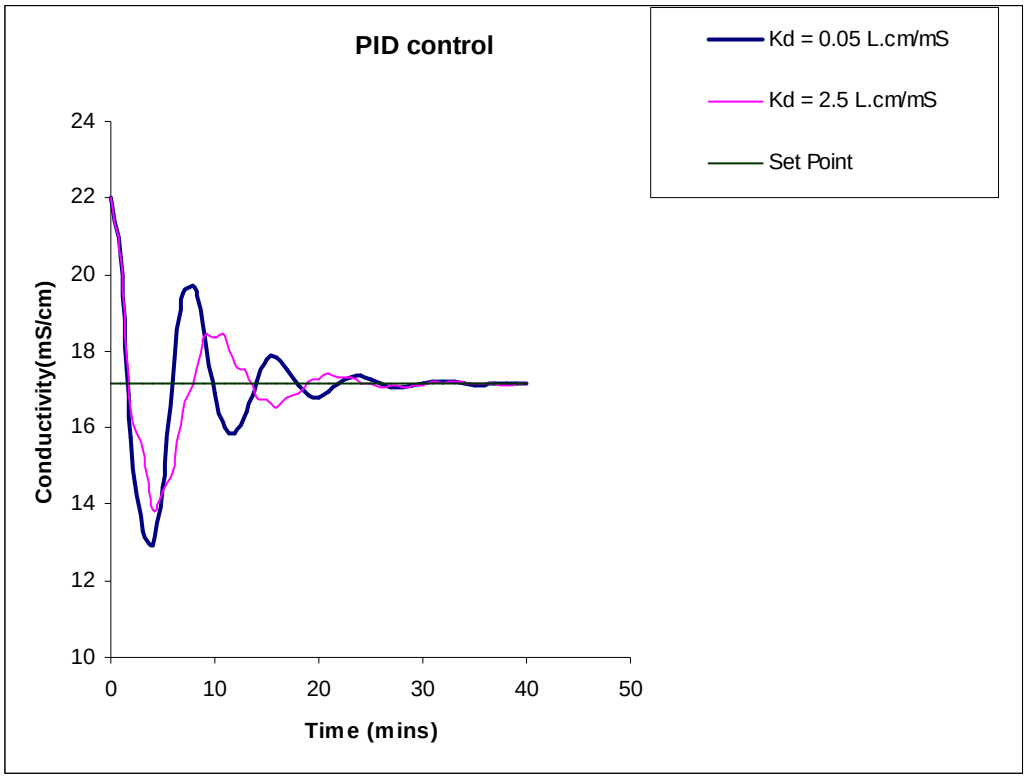

Figure 3.8: Plot of conductivity of stage 6 eluate buffer over time using PI control for different K_ds

In figure 3.8, as K_d reaches the higher value of 2.5 L.cm/mS small oscillations (along with the bigger ones) begin to be visible. So over all in order to implement PID control at Bayer, the best combination of K_p, K_I and K_d with the optimum flow rate will have to be established in the future.

Chapter 4: Conclusion and Future Work

Chapter one describes a pH adjustment automation step for the stage 6 eluate buffer before it enters the next chromatographic column. Even though the pH adjustment process was developed successfully in the first chapter, it lacked a base predictive pH model which was developed later in chapter two. In the future, a feedback controlled automation process should be developed that uses the model developed in chapter two to predict the pH on the following lines:

The H^+ ion concentration was calculated in chapter two as follows:

$$[H^+] = \frac{-K_a + \sqrt{K_a{}^2 + 4K_aC_a}}{2} \tag{4.1}$$

C_a in the above equation can be obtained from equation (2.27)

$$C_a = \frac{0.27 \times (Total\ Histidine\ added)}{V + (Total\ Histidine\ added)}$$

$$C_a = \frac{0.27 \times (\int F(t)dt)}{V + (\int F(t)dt)} \tag{4.2}$$

C_a from equation (4.2) can be plugged into equation (4.1) and the following equation can be obtained:

$$H^+(t) = \frac{-K_a + \sqrt{K_a{}^2 + 4K_a \times 0.27 \frac{\int F(t)dt}{V + \int F(t)dt}}}{2} \tag{4.3}$$

Here *F(t)* can be calculated based on P, PI or PID control model depending on the desired algorithm. PID control equation for the flow rate is shown as follows:

$$F(t) = K_p \times (H^+_{sp} - H^+(t)) + K_I \int_0^t (H^+_{sp} - H^+(t)) \quad + K_d \frac{d}{dt}(H^+_{sp} - H^+(t)) \qquad (4.4)$$

Future work should be done on these lines and the most optimum control model should be developed with the aim of fully automating the pH adjustment process.

Similarly, using Kohlrausch's model, an automated process should be developed to predict the conductivity of the SP eluate solution. As described in the equations above, $\lambda(t)$ can be written in terms of Kohlrausch's model as show in equation (4.5):

$$\lambda(t) = \lambda_\infty - K\sqrt{\frac{1}{m_t}} \qquad (4.5)$$

Here m_t is the instantaneous mass of the solution that can be obtained by doing a mass balance on the SP eluate tank as follows:

Accumulation = Input – Output + Generation – Consumption

$$\frac{dm_t}{dt} = F_{in} - 0 + 0 - 0 \qquad (4.6)$$

Equation (4.5) can be rearranged to evaluate m_t as shown in the following equation

$$m_t = \frac{K^2}{(\lambda_\infty - \lambda(t)^2} \qquad (4.7)$$

m_t can be replaced in equation (4.6) using equation (4.7). Rearranging the equation and solving for $\frac{d\lambda}{dt}$, equation (4.8) is obtained:

$$\frac{d}{dt}\left(\frac{K^2}{(\lambda_\infty - \lambda(t))^2}\right) = F_{in}$$

$$\frac{d\lambda(t)}{dt} = \frac{(\lambda_{\infty} - \lambda)^3 F_{in}}{2K^2} \tag{4.8}$$

Equation (4.8) represents the rate of change of conductivity over time. This equation can now be used to derive the control equation for the amount of WFI to be added based on the instantaneous conductivity. The governing equation for the control model could again be written in terms of proportional control, proportional integral control or proportional integral derivative control. Equation (4.9) presents the WFI flow rate equation in terms of PID control:

$$F(t) = K_p \times (\lambda(t) - \lambda_{sp}) + \mathrm{K_I} \int_0^t \lambda(\mathrm{t}) - \lambda_{sp}) \quad + \mathrm{K_d} \frac{d(\lambda(t) - \lambda_{\mathrm{sp}})}{dt} \tag{4.9}$$

Equation (4.9) and (4.8) can be combined to obtain equation (4.10):

$$\frac{d\lambda(t)}{dt} = \frac{(\lambda_{\infty} - \lambda(t))^3 (K_p \times (\lambda(t) - \lambda_{sp}) + \mathrm{K_I} \int_0^t \lambda(\mathrm{t}) - \lambda_{sp}) + \mathrm{K_d} \frac{d(\lambda(t) - \lambda_{\mathrm{sp}})}{dt}}{2K^2} \tag{4.10}$$

Equation (4.10) can be integrated numerically and the conductivity could be obtained over time. The control gain coefficients can be fine tuned experimentally and the most optimum model with the least error could be developed.

Even though it would be very efficient to have a fully automated pH and conductivity adjustment process, due to the extremely expensive nature of the drug at this step there is no tolerance for over dilution with WFI or histidine. Hence, it is important to have manual checks, as developed in the automation algorithm in chapter one in order to make sure that the calculated histidine or WFI values are not unreasonably high. Also, in a case of DCS glitch or a system failure, operator presence would be of paramount importance in preventing over-addition of histidine or WFI.

Even though the operators are indispensable for this critical pH/conductivity adjustment step, the automation will definitely reduce the number of operators from two full time operators to one part time operator. Also, the addition would be much more accurate and precise and the experimental values will be repeatable barring human error.

Along with the theoretical pH and conductivity predictive models developed in this project, past histidine and WFI data should be analyzed and empirical correlations should be developed relating WFI and histidine with conductivity and pH. These correlations should be used in tandem with the theoretical models to ensure maximum accuracy.

Over all the project has explored the automation of histidine pH and conductivity adjustment process in a great detail. This work would definitely be a significant stepping stone in the development of a much more robust and sophisticated model in the future.

Bibliography

[1]Anderko, Andrez, and Malgorzata M. Lencka. "Computation of Electrical Conductivity of Multicomponent Aqueous Systems in Wide Concentration and Temperature Ranges." *Industrial and Engineering Chemistry Research* 36 (1997): 1932-943. Web. 04 Jan. 2010.

[2] Bayer Healthcare, “Process Description: Purification”, Berkeley, CA, 2006

[3] Bayer Healthcare, “Batch Production Record for Stage 6 Column Eluate”, Berkeley, CA, 2006

[4] Castellan, Gilbert William. "Electrical Conduction." *Physical Chemistry*. 3rd ed. Reading, Mass.: Addison-Wesley, 1983. p773.

[5] Harris, Daniel C. *Exploring Chemical Analysis*. 6th ed. New York: W.H. Freeman, 2005. p185.

[6] Harris, Daniel C. "Polyprotic Acid Base Equilibria." *Quantitative Chemical Analysis*. 6th ed. New York: W.H. Freeman and, 2003. p 213.

[7] Harris, Daniel C. *Quantitative Chemical Analysis*. 6th ed. Michelle Russel Julet, 2003.

[8] Jones, Harry Clary. *The Theory of Electrolytic Dissociation and Some of Its Applications.* 3rd ed. New York: Macmillanmpany, 1906.

[9] Kim, Cherng-ju. *Advanced Pharmaceutics: Physiochemical Principles*. Boca Raton (Fla.): CRC, 2004.

[10]National Institute of Standards and Technology (U.S.). *NIST*. Gaithersburg, Md.: U.S. Dept. ofmmerce, National Institute of Standards and Technology, 2008.

NIST Standard Reference Database 69. Web. 04 Apr. 2010. <http://webbook.nist.gov/ >.

[11] Riggs, James B. "PID Control." *Chemical Process Control*. 2nd ed. Lubbock, Tex.: Ferret, 2001. 232.

[12] Romagnoli, Jose? A., and Ahmet Palazog?lu. "Basic Elements of Feedback Control." *Introduction to Process Control*. Boca Raton, FL: Taylor & Francis/CRC, 2006. p 165.

[13] Seborg, Dale E., Thomas F. Edgar, and Duncan A. Mellichamp. "Feedback Controllers." *Process Dynamics and Control*. New York: Wiley, 1989. 191.

[14] Smith, Carlos A. *Automated Continuous Process Control*. New York: J. Wiley, 2002. p 41.

[15] Triana, Jonathan R., Mark Yanagihashi, and Douglas F. Larson. "Mathematical modeling of buffers used in myocardial preservation." *Perfusion* 22.5 (2007): 353-362. *Academic Search Premier*. EBSCO. Web. 4 Apr. 2010

[16] Boeve, Lucas. Method of Producing Ultrapure Pyrogen-free Water. Patent 4548756. 22 Oct. 1985. Print.